

Research Article

Nayak G, et al. J Pharma Pharma Sci 04: JPPS-178.
DOI: 10.29011/2574-7711.100078

Complementary and Alternative Medicine: Impact of Consciousness Healing Treatment on the Characteristic Properties of Sulfamethoxazole

Gopal Nayak¹, Mahendra Kumar Trivedi¹, Alice Branton¹, Dahryn Trivedi¹ and Snehasis Jana^{2*}

¹Trivedi Global, Inc., Henderson, USA

²Trivedi Science Research Laboratory Pvt. Ltd., Bhopal, India

***Corresponding author:** Snehasis Jana, Trivedi Science Research Laboratory Pvt. Ltd., Bhopal, India. Tel: +91-022-25811234; Email: publication@trivedieffect.com

Citation: Nayak G, Trivedi MK, Branton A, Tivedi D, Jana S (2019) Complementary and Alternative Medicine: Impact of Consciousness Healing Treatment on the Characteristic Properties of Sulfamethoxazole. J Pharma Pharma Sci 04: 179. DOI: 10.29011/2574-7711.100079

Received Date: 20 March 2019; **Accepted Date:** 05 April 2019; **Published Date:** 16 April, 2019

Abstract

Sulfamethoxazole is the sulfonamide class of antibiotic that acts as a bacteriostatic agent against various bacteria. The current study was aimed to analyze the impact of the Consciousness Energy Healing Treatment (the Trivedi Effect[®]) on various properties of sulfamethoxazole by using different modern analytical techniques. For this, the sample was first divided into two parts, followed by considering one part as a control sample (no treatment was given). The second part was named as the Biofield Energy Treated sample that was remotely given the Consciousness Energy Healing Treatment by a renowned Biofield Energy Healer, Gopal Nayak. The particle size values were reduced by 14.35%(d_{10}), 8.93%(d_{50}), 7.84%(d_{90}), and 9.24%{D(4,3)}; therefore, the specific surface area was increased by 9.68% in the treated sample compared to the control sample. The PXRD peak intensities and crystallite sizes were significantly altered ranging from -68.71% to 40.38% and -31.58% to 169.60%, respectively; however, the average crystallite size was significantly increased by 9.49% in the treated sample compared to the control sample. The residue weight and maximum thermal degradation temperature were increased by 2.12% and 3.25%, respectively in the treated sample compared with the control sample. The decomposition temperature, latent heat of fusion, and latent heat of decomposition were significantly increased by 11.44%, 48.27%, and 22.59%, respectively in the treated sample compared to the control sample. Thus, the Trivedi Effect[®]-Consciousness Energy Healing Treated sulfamethoxazole might have formed a new polymorph with reduced particle size and improved surface area and thermal stability. Hence, the use of the treated sulfamethoxazole might be more beneficial in terms of improved solubility, absorption, bioavailability, stability and also for designing the more efficacious pharmaceutical formulations for the treatment and prevention of various bacterial diseases, i.e., ear infections, urinary tract infections, shigellosis, traveler's diarrhea, bronchitis, and pneumocystis-type of pneumonia, etc.

Keywords: Complementary and alternative medicine; Consciousness energy healing treatment; DSC; Particle size; PXRD; Sulfamethoxazole; The Trivedi Effect[®]

Introduction

Sulfamethoxazole belongs to the sulphonamides group of antibiotics that is a structural analog of *p*-aminobenzoic acid (PABA). Sulfamethoxazole inhibits the growth of bacteria by competing with PABA and get bind to dihydropteroate synthetase in place of PABA and thereby inhibit the formation of dihydrofolic acid [1]. Such inhibition of the dihydrofolate formation further

interferes with the bacterial synthesis of folate. Folate acts as an essential metabolite that is responsible for the growth and replication of bacteria. Thus, its blockage inhibits the bacterial growth by inhibiting the metabolic processes; therefore, sulfamethoxazole acts as a bacteriostatic antibiotic [2,3]. It is used in combination with trimethoprim in the treatment of various bacterial infections such as respiratory, middle ear, intestinal, and urine infections, traveler's diarrhoea, shigellosis, etc. Moreover, its use is also evident in the prevention and treatment of pneumocystis-type of pneumonia [4].

Although, sulfamethoxazole has rapid oral absorption; however approximately 70% of it is in plasma protein-bound form. Besides, the bioavailability and performance of any drug are based on its analytical and stability profile [5]. In this regard, the efforts were done to improve the physicochemical and thermal profile of the drugs such as particle size, surface area, polymorphic form, and thermal decomposition, etc. By altering such parameters, one can easily achieve a formulation with maximum biological activities [6,7]. The Trivedi Effect®-Consciousness Energy Healing Treatment is also known for its significant role in modifying the structural, physical, and thermal properties of several compounds in various research studies [8,9]. Biofield Energy Healing is an Energy Therapy that is known for its use to fighting against various diseases and was accepted by National Center for Complementary and Alternative Medicine (NCCAM) [10,11] under the Complementary and Alternative Medicine (CAM) therapies. Therefore, it is suggested that a human has the ability to harness energy from the universe and it could be transmitted to any living organism(s) or non-living object(s) around the globe. The impact of the Biofield Energy Healing Treatment has been already reported in various studies for causing a significant alteration in the physicochemical and thermal properties of metals [12,13], organic compounds, pharmaceuticals, nutraceuticals [14-17], and polymers [18], affecting the antimicrobial activity [19-21], agricultural productivity [22,23], enhancing the bioavailability [24-26], and improving the skin and bone health [27-30]. Therefore, this study was carried out to analyse the effect of the Trivedi Effect® on the physicochemical and thermal properties of sulfamethoxazole by using various analytical techniques.

Materials and Methods

Chemicals and Reagents

Sulfamethoxazole was purchased from Sigma Aldrich, the USA and the other chemicals were purchased in India.

Consciousness Energy Healing Treatment Strategies

The experiment involved dividing the sulfamethoxazole sample into two equal parts. The first part was considered as a control sample and it was not received the Biofield Energy Treatment. However, the second part of the sample was received the Trivedi Effect®-Energy of Consciousness Healing Treatment remotely under standard laboratory conditions for 3 minutes and known as The Biofield Energy Treated sample. This Biofield Energy Treatment was provided by the renowned Biofield Energy Healer, Gopal Nayak, India, through the unique energy transmission

process, to the test sample. Further, the control sample was treated with a “sham” healer for comparison purpose, where the sham healer did not have any knowledge about the Biofield Energy Treatment. Later on, both the samples were kept in sealed conditions and characterized using PSA, PXRD, TGA, and DSC techniques.

Characterization

The PSA, PXRD, TGA, and DSC analysis of sulfamethoxazole were performed. The PSA was performed with the help of Malvern Mastersizer 2000 (the UK) using the wet method [31,32]. The PXRD analysis of sulfamethoxazole powder sample was performed with the help of Rigaku MiniFlex-II Desktop X-ray diffractometer (Japan) [33,34]. The average size of crystallites was calculated from PXRD data using the Scherrer's formula (1)

$$G = k\lambda/\beta\cos\theta \quad (1)$$

Where G is the crystallite size in nm, k is the equipment constant (0.94), λ is the radiation wavelength (0.154056 nm for $K\alpha_1$ emission), β is the full-width at half maximum, and θ is the Bragg angle [35].

The TGA/DTG analysis of sulfamethoxazole was performed with the help of TGA Q50 TA Instruments. Similarly, the DSC analysis was performed with the help of DSC Q200, TA Instruments [16].

The % change in particle size, Specific Surface Area (SSA), peak intensity, crystallite size, melting point, latent heat, weight loss, and the maximum thermal degradation temperature (T_{max}) of the Biofield Energy Treated sample was calculated compared with the control sample using the following equation 2:

$$\% \text{ change} = \frac{[\text{Treated} - \text{Control}]}{\text{Control}} \times 100 \quad (2)$$

Results and Discussion

Particle Size Analysis (PSA)

The particle size distribution corresponding to d_{10} , d_{50} , d_{90} , and $D(4, 3)$ were analysed for the control and treated samples and the results are mentioned in Table 1. The comparative analysis of particle size distribution between the control and treated sulfamethoxazole samples revealed the significant reduction in the particle size values of the treated sample after the Biofield Energy Treatment with respect to the control sample. The particle sizes of treated sample were decreased at d_{10} , d_{50} , d_{90} , and $D(4, 3)$ by 14.35%, 8.93%, 7.84%, and 9.24%, respectively as compared to the control sample.

Parameter	d_{10} (μm)	d_{50} (μm)	d_{90} (μm)	$D(4,3)$ (μm)	SSA(m^2/g)
Control	14.49	46.15	101.36	53.02	0.31
Biofield Treated	12.41	42.03	93.41	48.12	0.34
Percent change* (%)	-14.35	-8.93	-7.84	-9.24	9.68

d_{10} , d_{50} , and d_{90} : particle diameter corresponding to 10%, 50%, and 90% of the cumulative distribution, $D(4,3)$: the average mass-volume diameter, and SSA: the specific surface area.

Table 1: Particle size distribution of the control and Biofield Energy Treated sulfamethoxazole.

Moreover, the significant decrease in the particle size values further affected the specific surface area of the treated sulfamethoxazole sample whose surface area ($0.34\ m^2/g$) was increased by 9.68% compared with the SSA of the control sample ($0.31\ m^2/g$). The observed changes might occur as Biofield Energy Treatment might exert some force on the treated sample that possibly reduces the particle sizes of sulfamethoxazole. The smaller particle size and increased surface area may help in increasing the dissolution and absorption of the drug and thus, may improve the bioavailability of the drug [36,37]. Thus, it is presumed that the bioavailability profile of the treated sulfamethoxazole might be improved after the Biofield Energy Treatment, compared to the untreated sample.

Powder X-Ray Diffraction (PXRD) Analysis

The PXRD diffractograms of the control and treated samples are shown in Figure 1 and the corresponding data are presented in Table 2. There was the presence of sharp and intense peaks in the diffractograms of both the samples that represented their crystalline nature.

Entry No.	Bragg angle ($^{\circ}2\theta$)		Intensity (cps)			Crystallite size (G, nm)		
	Control	Treated	Control	Treated	% change	Control	Treated	% change
1	6.92	6.82	163	51	-68.71	526	471	-10.46
2	12.40	12.32	286	249	-12.94	359	389	8.36
3	13.83	13.76	115	114	-0.87	333	345	3.60
4	17.05	16.97	127	44	-65.35	250	674	169.60
5	17.57	17.45	265	372	40.38	386	445	15.28
6	18.64	18.55	133	129	-3.01	380	439	15.53
7	19.70	19.62	115	93	-19.13	354	384	8.47
8	20.76	20.72	971	835	-14.01	408	402	-1.47
9	21.62	21.56	306	268	-12.42	363	406	11.85
10	22.47	22.41	207	189	-8.70	411	402	-2.19
11	23.97	23.88	797	707	-11.29	292	274	-6.16
12	24.77	24.68	162	135	-16.67	236	248	5.08
13	27.52	27.44	303	337	11.22	356	394	10.67
14	28.85	28.76	185	178	-3.78	362	380	4.97
15	32.27	32.22	193	206	6.74	322	301	-6.52
16	35.10	34.99	60	81	35.00	266	182	-31.58

Table 2: PXRD data for the control and Biofield Energy Treated sulfamethoxazole.

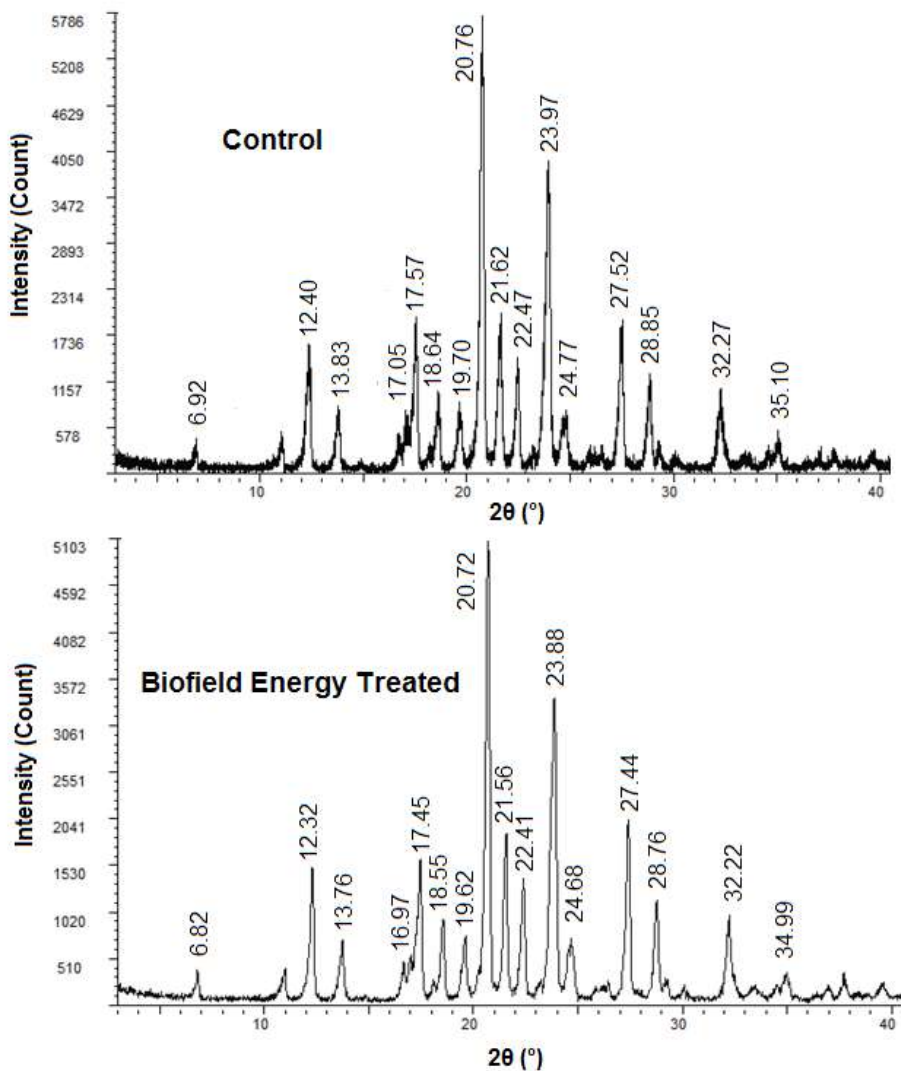


Figure 1: PXRD diffractograms of the control and Biofield Energy Treated sulfamethoxazole.

The results of the PXRD data showed slight alterations between the Bragg's angles of the peaks of the control and treated samples (Table 2). The peak intensities corresponding to the characteristic peaks of the treated sulfamethoxazole sample showed significant changes ranging from -68.71% to 40.38% in comparison to the control sample. Similarly, the crystallite sizes on the various plane of the treated sample also showed variation with respect to the control sample. The crystallite sizes were altered ranging from -31.58% to 169.60% after the Biofield Energy Treatment compared to the control sample. Moreover, the Biofield Energy Treatment also altered the average crystallite size of the treated sample (383.50 nm) that was increased by 9.49% compared with the control sample (350.25 nm).

The significant changes in the peak intensities of the treated sample might be indicative of the possible alterations in the crystallinity in comparison to the untreated one. Moreover, the peak intensities and crystallite sizes corresponding to various plane decide the polymorphic form of the compound, which ultimately affects the drug performance [38,39]. Thus, it could be anticipated that the significant alterations taken place regarding the peak intensities and crystallite size of the treated sample might occur as a result of a novel polymorph formation after the Biofield Energy Treatment that may also help in improving the drug profile of the treated sulfamethoxazole as compared to the untreated sample.

Thermal Gravimetric Analysis (TGA)/ Differential Thermogravimetric Analysis (DTG)

The thermogravimetric analysis of both the samples was used to determine any difference in the thermal stability profile of the treated sample after the Biofield Energy Treatment. The TGA thermogram of the treated sulfamethoxazole showed a reduction in the total weight loss of 1.09% during the heating of the sample compared to the control sample. Therefore, the residue weight of the Biofield Energy Treated sample was increased by 2.12% (Table 3) in comparison to the control sample. Thus, it is presumed that the thermal stability of the treated sample was improved after the Biofield Energy Treatment compared to the untreated sample.

Besides, the DTG thermograms of both the samples (Figure 3) showed two peaks. The first maximum thermal degradation temperature (T_{max}) was observed at 250.78°C while it was increased up to 258.94°C for the treated sample. Thus, the T_{max} observed from the first peak of the treated sample was increased by 3.25%; while the T_{max} corresponding to the second peak was slightly reduced as compared to the control sample. Overall, the TGA/DTG results indicated the improved thermal stability of the treated sample after the Biofield Energy Treatment compared with the untreated sulfamethoxazole sample.

Sample	TGA		DTG { T_{max} (°C)}	
	Total weight loss (%)	Residue %	Peak 1	Peak 2
Control	67.01	32.99	250.78	321.16
Biofield Energy Treated	66.28	33.72	258.94	321.00
% Change	-1.09	2.12	3.25	-0.05

T_{max} = the temperature at which maximum weight loss takes place in TG or peak temperature in DTG.

Table 3: TGA/DTG data of the control and Biofield Energy Treated samples of sulfamethoxazole.

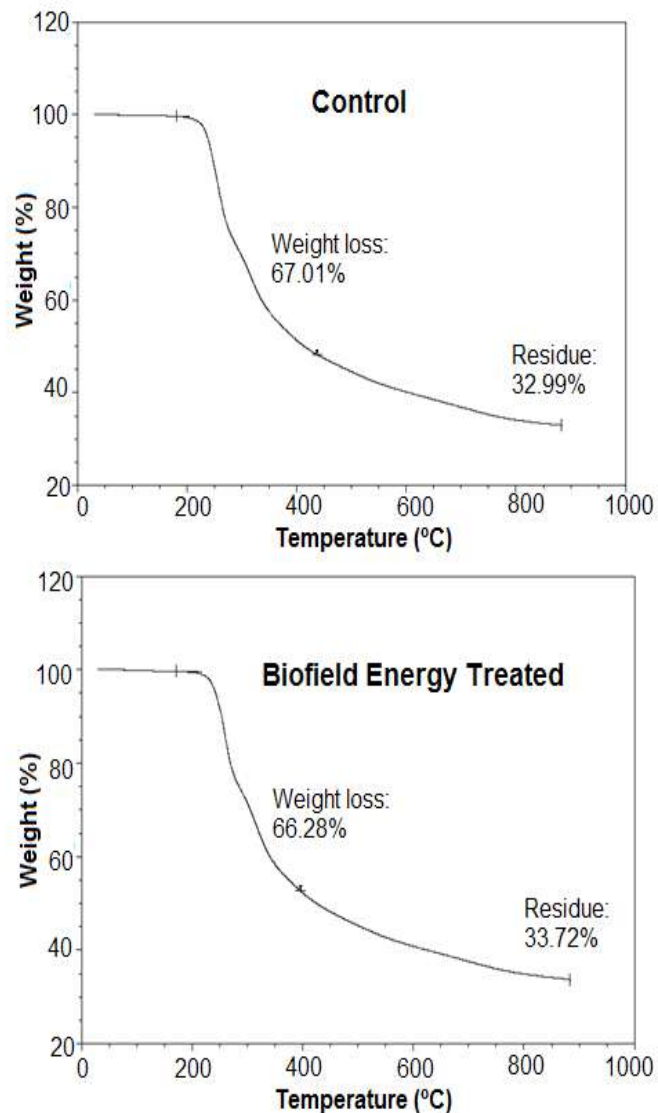


Figure 2: TGA thermograms of the control and Biofield Energy Treated sulfamethoxazole.

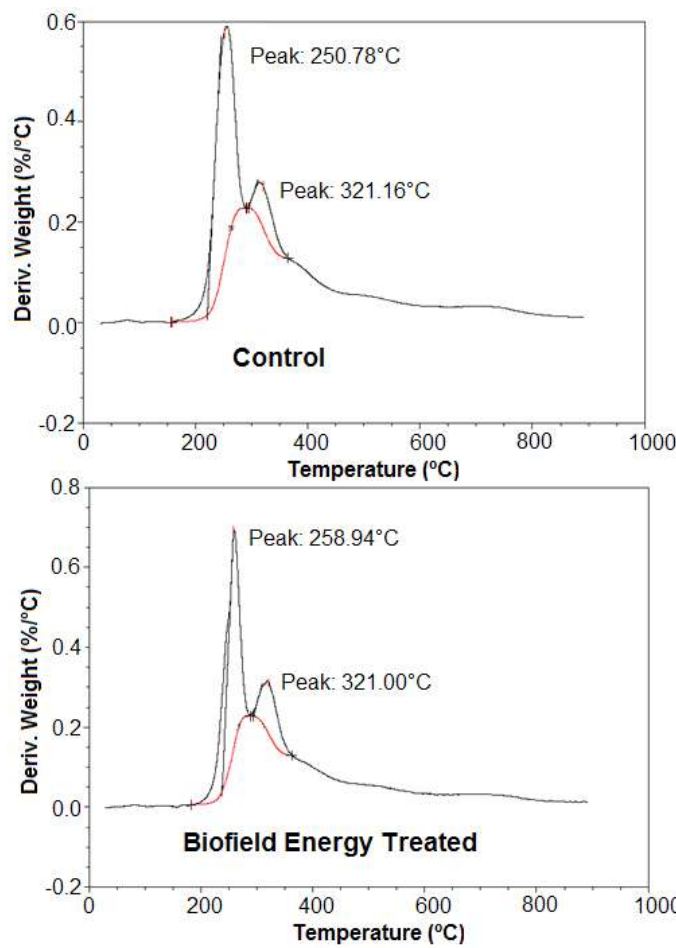


Figure 3: DTG thermograms of the control and Biofield Energy Treated sulfamethoxazole.

Differential Scanning Calorimetry (DSC) Analysis

The DSC analysis helps in studying the difference in the melting, crystallization and thermal behaviour [37] of the treated sample after the Biofield Energy Treatment in comparison to the untreated one. The previous studies on sulfamethoxazole revealed presence of two peaks in the DSC thermogram; among which, the first peak was endothermic peak (observed near 172°C) and denotes the fusion process; while, the second peak was observed to be exothermic in nature and shows the oxidation of evolved products or the thermal degradation of the sample. The DSC thermograms (Figure 4) of both the samples, i.e., the control and the treated samples were observed similarly as reported in the literature [40]. The melting peak of the control and the treated samples were observed at 170.52°C and 171.53°C, respectively (Table 4). Thus, the melting point of the treated sample was slightly increased by 0.59% compared to the control sample. The latent heat of fusion (ΔH) of the treated sample (181.48 J/g) was

also significantly increased by 48.27% compared to the ΔH_{fusion} of the control sample (122.4 J/g).

Peak	Description	Melting Point (°C)	ΔH (J/g)
Peak 1	Control sample	170.52	122.4
	Biofield Treated sample	171.53	181.48
	% Change	0.59	48.27
Peak 2	Control sample	250.9	565.7
	Biofield Treated sample	279.61	693.5
	% Change	11.44	22.59

ΔH : Latent heat of fusion/ decomposition.

Table 4: Comparison of DSC data between the control and Biofield Energy Treated sulfamethoxazole.

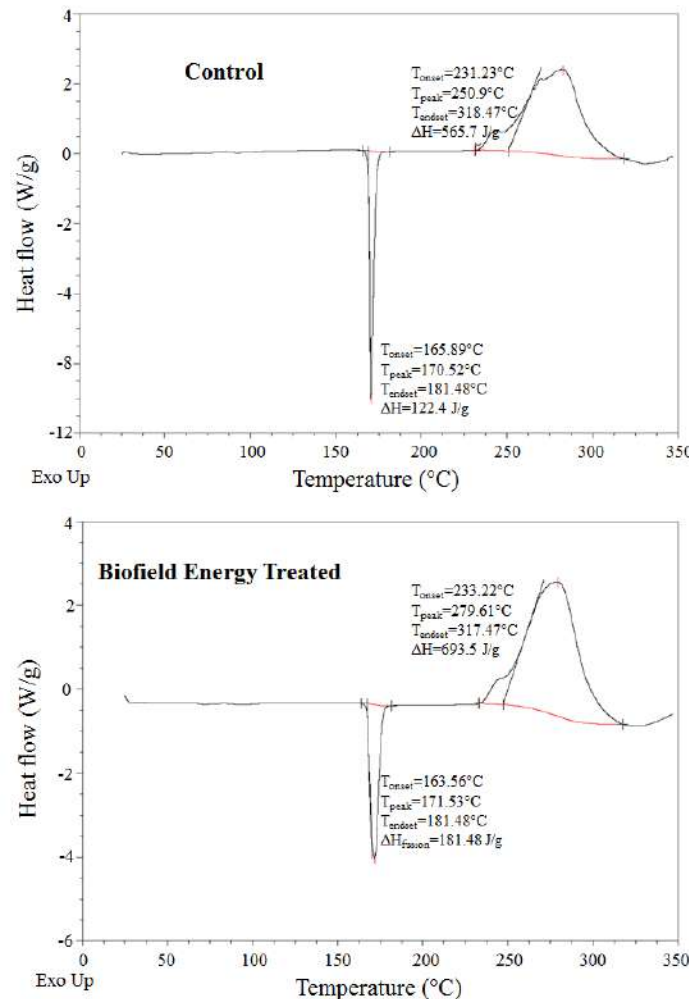


Figure 4: DSC thermograms of the control and Biofield Energy Treated sulfamethoxazole.

Besides, the broad exothermic inflection in the DSC thermogram of the treated sample was observed at 279.61°C that was increased by 11.44% in comparison to the peak of the control sample (250.9°C) along with 22.59% significant improvement in the $\Delta H_{\text{decomposition}}$. Hence, it showed a significant improvement in the decomposition temperature of the treated sample after the Biofield Energy Treatment compared with the untreated sulfamethoxazole sample. Therefore, the results indicate the improved thermal stability of the Biofield Energy Treated sample in comparison to the control sample that might occur due to alterations in the molecular chains and crystallization structure of the treated sample.

Conclusions

The study helped in analyzing the influence of the Trivedi Effect®-Consciousness Energy Healing Treatment on the physicochemical and thermal properties of sulfamethoxazole. The Biofield Energy Treated sample showed a reduction in their particle size values at d_{10} , d_{50} , d_{90} , and $D(4,3)$ by 14.35%, 8.93%, 7.84%, and 9.24%, respectively compared with the untreated sample. The resultant change was also observed in the specific surface area of the treated sulfamethoxazole sample that was significantly increased by 9.24% as compared to the control sample. Such significant changes in the particle size distribution might be helpful in improving the solubility and absorption of the treated sulfamethoxazole sample in comparison to the control sample. The PXRD data indicated the crystalline nature of both the samples however the Bragg's angles of the characteristic peaks of the treated sample differ from the control sample. Also, the Biofield Energy Treated sample showed alterations in the peak intensities ranging from -68.71% to 40.38% along with -31.58% to 169.60% changes in the crystallite sizes as compared to the untreated sample. Moreover, the average crystallite size of the treated sample was increased by 9.49% after the Biofield Energy Treatment as compared to the control sample. The residue weight and the T_{max} was increased by 2.12% and 3.25%, respectively in the treated sample compared with the control sample. The decomposition temperature, ΔH_{fusion} , and $\Delta H_{\text{decomposition}}$ were significantly increased by 11.44%, 48.27%, and 22.59%, respectively in the treated sample compared to the control sample. Thus, the TGA/DTG and DSC data indicated the improved thermal stability of the treated sulfamethoxazole sample after the Biofield Energy Treatment compared to the untreated sample. Therefore, the study concluded the significant effect of the Trivedi Effect®-Consciousness Energy Healing Treatment on the physicochemical and thermal properties of sulfamethoxazole. The Biofield Energy Treatment might help in forming a new polymorph of sulfamethoxazole, which may have improved bioavailability and thermal stability compared with the untreated sample. Hence, the Consciousness Energy Healing Treated sulfamethoxazole might be considered to play a better role in the treatment and prevention of various bacterial diseases such

as ear infections, urinary tract infections, shigellosis, traveler's diarrhea, bronchitis, and pneumocystis-type of pneumonia, etc.

Acknowledgements

The authors are grateful to Central Leather Research Institute, SIPRA Lab. Ltd., Trivedi Science, Trivedi Global, Inc., Trivedi Testimonials, and Trivedi Master Wellness for their assistance and support during this work.

References

1. Neu HC, Gootz TD (1996) Antimicrobial Chemotherapy. In: Medical Microbiology. 4th Edition. Baron S (Editor). University of Texas Medical Branch at Galveston, Galveston TX, USA.
2. Zander J, Besier S, Ackermann H, Wichelhaus TA (2010) Synergistic Antimicrobial Activities of Folic Acid Antagonists and Nucleoside Analogs. *Antimicrob Agents Chemother* 54: 1226-1231.
3. Brunton L, Chabner BA, Knollman B (2011) Goodman and Gilman's The Pharmacological Basis of Therapeutics. 12th Edition., The McGraw-Hill Companies, Inc., USA.
4. Close SJ, McBurney CR, Garvin CG, Chen DC, Martin SJ (2002) Trimethoprim-sulfamethoxazole activity and pharmacodynamics against glycopeptide-intermediate *Staphylococcus aureus*. *Pharmaco-therapy* 22: 983-989.
5. Mulla SI, Hu A, Sun Q, Li J, Suanon F, et al. (2018) Biodegradation of sulfamethoxazole in bacteria from three different origins. *J Environ Manage* 206: 93-102.
6. Khadka P, Ro J, Kim H, Kim I, Kim JT, et al. (2014) Pharmaceutical particle technologies: An approach to improve drug solubility, dissolution and bioavailability. *Asian J Pharm* 9: 304-316.
7. Savjani KT, Gajjar AK, Savjani JK (2012) Drug solubility: importance and enhancement techniques. *ISRN Pharm* 2012: 195727.
8. Trivedi MK, Branton A, Trivedi D, Nayak G, Plikerd WD, et al. (2017) Evaluation of the physicochemical, spectral, thermal and behavioral properties of sodium selenate: influence of the energy of consciousness healing treatment. *American Journal of Quantum Chemistry and Molecular Spectroscopy* 1: 31-40.
9. Trivedi MK, Mohan TRR (2016) Biofield energy signals, energy transmission and neutrinos. *American Journal of Modern Physics* 5: 172-176.
10. Koithan M (2009) Introducing complementary and alternative therapies. *J Nurse Pract* 5: 18-20.
11. Hintz KJ, Yount GL, Kadar I, Schwartz G, Hammerschlag R, et al. (2003) Bioenergy definitions and research guidelines. *Altern Ther Health Med* 9: A13-A30.
12. Trivedi MK, Tallapragada RM (2008) A transcendental to changing metal powder characteristics. *Met Powder Rep* 63: 22-28, 31.
13. Trivedi MK, Nayak G, Patil S, Tallapragada RM, Latiyal O (2015) Studies of the atomic and crystalline characteristics of ceramic oxide nano powders after bio field treatment. *Ind Eng Manage* 4: 161.
14. Trivedi MK, Branton A, Trivedi D, Nayak G, Bairwa K, et al. (2015) Spectroscopic characterization of disodium hydrogen orthophosphate and sodium nitrate after biofield treatment. *J Chromatogr Sep Tech* 6: 282.

15. Trivedi MK, Branton A, Trivedi D, Nayak G, Panda P, et al. (2016) Evaluation of the isotopic abundance ratio in biofield energy treated resorcinol using gas chromatography-mass spectrometry technique. *Pharm Anal Acta* 7: 481.
16. Trivedi MK, Branton A, Trivedi D, Nayak G, Plikerd WD, et al. (2017) A systematic study of the biofield energy healing treatment on physico-chemical, thermal, structural, and behavioral properties of Magnesium Gluconate. *International Journal of Bioorganic Chemistry*. 2: 135-145.
17. Trivedi MK, Branton A, Trivedi D, Nayak G, Plikerd WD, et al. (2017) Chromatographic and spectroscopic characterization of the consciousness energy healing treated *Withania somnifera* (ashwagandha) root extract. *European Journal of Biophysics* 5: 38-47.
18. Trivedi MK, Branton A, Trivedi D, Nayak G, Sethi KK, et al. (2016) Gas chromatography-mass spectrometry based isotopic abundance ratio analysis of biofield energy treated methyl-2-naphthylether (Nerolin). *American Journal of Physical Chemistry* 5: 80-86.
19. Trivedi MK, Branton A, Trivedi D, Nayak G, Charan S, et al. (2015) Phenotyping and 16S rDNA analysis after biofield treatment on *Citrobacter braakii*: A urinary pathogen. *J Clin Med Genomics* 3: 129.
20. Trivedi MK, Patil S, Shettigar H, Mondal SC, Jana S (2015) Evaluation of biofield modality on viral load of Hepatitis B and C viruses. *J Antivir Antiretrovir* 7: 83-88.
21. Trivedi MK, Patil S, Shettigar H, Mondal SC, Jana S (2015) An impact of biofield treatment: Antimycobacterial susceptibility potential using BACTEC 460/MGIT-TB System. *Mycobact Dis* 5: 189.
22. Trivedi MK, Branton A, Trivedi D, Nayak G, Mondal SC, et al. (2015) Morphological characterization, quality, yield and DNA fingerprinting of biofield energy treated alphonso mango (*Mangifera indica* L.). *Journal of Food and Nutrition Sciences* 3: 245-250.
23. Trivedi MK, Branton A, Trivedi D, Nayak G, Mondal SC, et al. (2015) Evaluation of biochemical marker-Glutathione and DNA fingerprinting of biofield energy treated *Oryza sativa*. *American Journal of BioScience* 3: 243-248.
24. Branton A, Jana S (2017) The influence of energy of consciousness healing treatment on low bioavailable resveratrol in male Sprague Dawley rats. *International Journal of Clinical and Developmental Anatomy* 3: 9-15.
25. Branton A, Jana S (2017) The use of novel and unique biofield energy healing treatment for the improvement of poorly bioavailable compound, berberine in male Sprague Dawley rats. *American Journal of Clinical and Experimental Medicine* 5: 138-144.
26. Branton A, Jana S (2017) Effect of the biofield energy healing treatment on the pharmacokinetics of 25-hydroxyvitamin D3 [25(OH)D3] in rats after a single oral dose of vitamin D3. *American Journal of Pharmacology and Phytotherapy* 2: 11-18.
27. Trivedi MK, Branton A, Trivedi D, Nayak G, Kinney JP, et al. (2017) Overall skin health potential of the biofield energy healing based herbomineral formulation using various skin parameters. *American Journal of Life Sciences* 5: 65-74.
28. Singh J, Trivedi MK, Branton A, Trivedi D, Nayak G, et al. (2017) Consciousness energy healing treatment based herbomineral formulation: A safe and effective approach for skin health. *American Journal of Pharmacology and Phytotherapy* 2: 1-10.
29. Ansari SA, Trivedi MK, Branton A, Trivedi D, Nayak G, et al. (2018) *In vitro* effects of biofield energy treated vitamin D3 supplementation on bone formation by osteoblasts cells. *Biomedical Sciences* 4: 10-17.
30. Koster DA, Trivedi MK, Branton A, Trivedi D, Nayak G, et al. (2018) Evaluation of biofield energy treated vitamin D3 on bone health parameters in human bone osteosarcoma cells (MG-63). *Biochemistry and Molecular Biology* 3: 6-14.
31. Trivedi MK, Sethi KK, Panda P, Jana S (2017) A comprehensive physicochemical, thermal, and spectroscopic characterization of zinc (II) chloride using X-ray diffraction, particle size distribution, differential scanning calorimetry, thermogravimetric analysis/differential thermogravimetric analysis, ultraviolet-visible, and Fourier transform-infrared spectroscopy. *Int J Pharm Investig* 7: 33-40.
32. Trivedi MK, Sethi KK, Panda P, Jana S (2017) Physicochemical, thermal and spectroscopic characterization of sodium selenate using XRD, PSD, DSC, TGA/DTG, UV-vis, and FT-IR. *Marmara Pharmaceutical Journal* 21: 311-318.
33. (1997) Desktop X-ray Diffractometer "MiniFlex". *The Rigaku Journal* 14: 29-36.
34. Zhang T, Paluch K, Scalabrino G, Frankish N, Healy AM, et al. (2015) Molecular structure studies of (1S,2S)-2-benzyl-2,3-dihydro-2-(1Hinden-2-yl)-1H-inden-1-ol. *J Mol Struct* 1083: 286-299.
35. Langford JI, Wilson AJC (1978) Scherrer after sixty years: A survey and some new results in the determination of crystallite size. *J Appl Cryst* 11: 102-113.
36. Mosharrof M, Nyström C (1995) The effect of particle size and shape on the surface specific dissolution rate of microsized practically insoluble drugs. *Int J Pharm* 122: 35-47.
37. Zhao Z, Xie M, Li Y, Chen A, Li G, et al. (2015) Formation of curcumin nanoparticles via solution enhanced dispersion by supercritical CO₂. *Int J Nanomedicine* 10: 3171-3181.
38. Trivedi MK, Branton A, Trivedi D, Nayak G, Lee AC, et al. (2017) Evaluation of the impact of biofield energy healing treatment (The Trivedi Effect®) on the physicochemical, thermal, structural, and behavioural properties of magnesium gluconate. *International Journal of Nutrition and Food Sciences* 6: 71-82.
39. Censi R, Di Martino P (2015) Polymorph Impact on the Bioavailability and Stability of Poorly Soluble Drugs. *Molecules* 20: 18759-18776.
40. Fernandes NS, Filho MASC, Mendes R, Ionashiro M (1999) Thermal decomposition of some chemotherapeutic substances. *J Braz Chem Soc* 10: 459-462.